**Response to the comments of Anonymous Referee #2**

We would like to thank anonymous referee#2 for the constructive feedback on our manuscript.
Our responses to the comments are shown below.
The comments of anonymous referee #2 are shown in black. Authors' responses are shown in blue.

---

The manuscript addresses commercial camera-based rainfall observation is a useful technology that contributes to the densification of rainfall observation networks. The study investigates the main and interactional effects of different commercial interval cameras (outdoor images) and rainfall intensity, which is interesting for measuring rainfall with high spatiotemporal resolution and low cost. The topic is important, and manuscript fits with the scope of the journal. but it has some weaknesses associated with the presented data and discussion have shortcomings as discussed below. Therefore, the current version of the manuscript needs major revision to be published in (HESS Journal). There are several issues must be addressed.

**Minor comments**

**< Comment 1 >**

- Regarding the title of manuscript, the title should show the novelty of the research and tell the main finding of the study. The title explains the problem... For example, you could write a title like this: "The effect of fluctuation and change in rainfall intensity when using commercial cameras on the accuracy of rainfall measurement"

Response:

We will revise the title as follows because the original title was unclear.

"Rainfall intensity estimations based on degradation characteristics of images taken with commercial cameras"

**Major comments**

**< Comment 2 >**

- For all tables and figures, no SD or SE. How the statistical analysis has been done with replicates. How many replicates are used for each camera? Please describe it in materials and methods section.

Response:

We will revise Figures 4, 5, 6, 7 and 11 with SD as follows. The revised Figures 4, 5, and 7 show the top three patches of scene depth for each camera. In terms of Figures 4, 5, and 7, we will move Figures which include all patches to an appendix C-1, C-2, and C-3.

As shown Table 1, there are multiple images at each rainfall intensity for each camera. SDs were calculated from these images. We will describe this in the captions of all figures with SD.

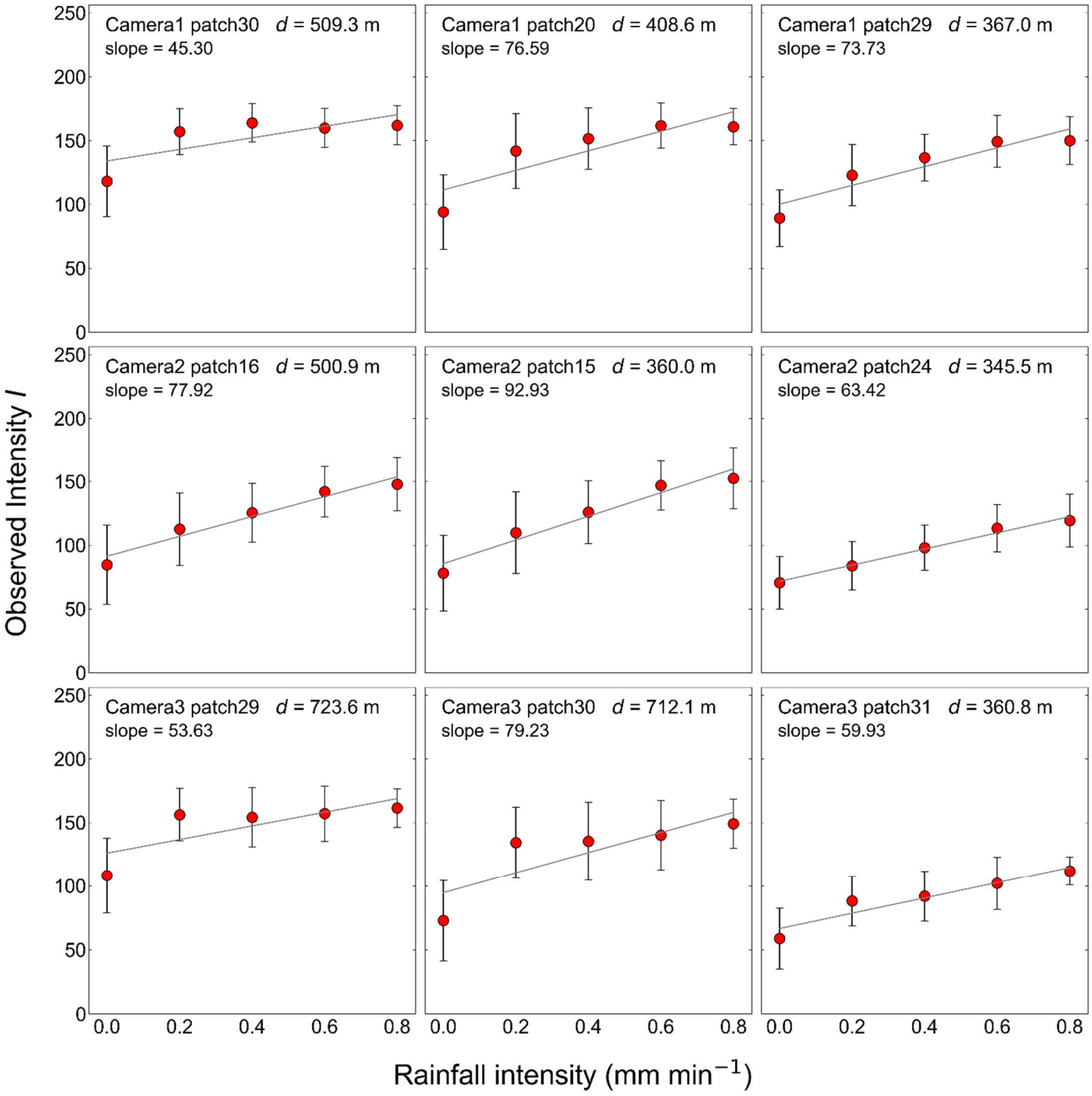


Figure 4. Distribution of observed intensity *I* by rainfall intensity. Figures show the top three patches of scene depth for each camera. Figures which include all patches are shown in Appendix C-1. Each figure is marked with a camera name, patch number, scene depth and slope of the linear regression line for the relationship between rainfall intensity and observed intensity *I*. The upper three figures are Camera 1, the middle three figures are Camera 2, and the lower three figures are Camera 3. The plots and error bars show the mean value and standard deviation of all data during the observation period. The straight lines show linear regression line for the relationship between rainfall intensity and observed intensity *I*. Rainfall intensity is observed by the rain gauge.

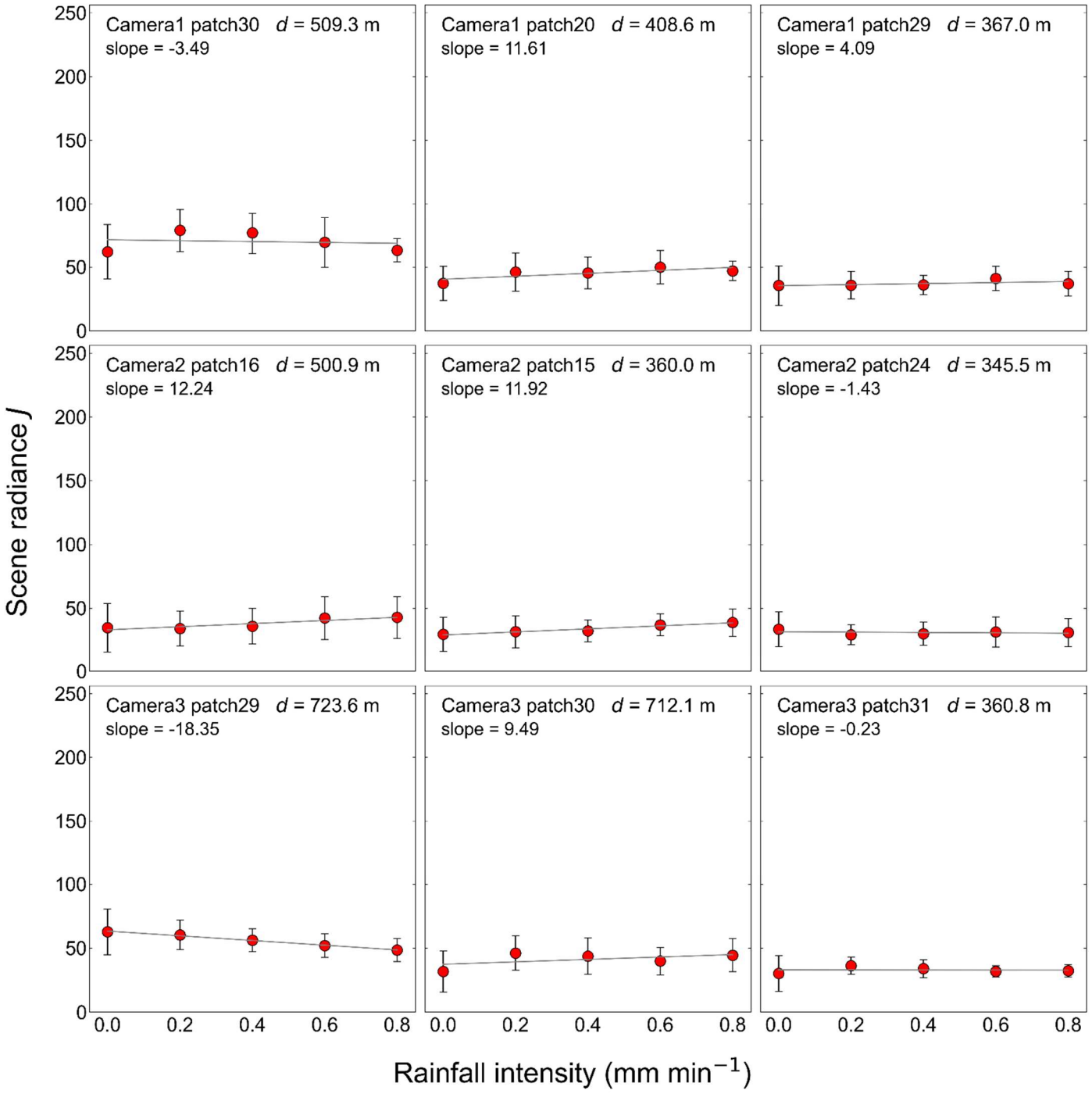


Figure 5. Distribution of scene radiance *J* by rainfall intensity. Figures show the top three patches of scene depth for each camera. Figures which include all patches are shown in Appendix C-2. Each figure is marked with a camera name, patch number, scene depth and slope of the linear regression line for the relationship between rainfall intensity and scene radiance *J*. The upper three figures are Camera 1, the middle three figures are Camera 2, and the lower three figures are Camera 3. The plots and error bars show the mean value and standard deviation of all data during the observation period. The straight lines show linear regression line for the relationship between rainfall intensity and scene radiance *J*. Rainfall intensity is observed by the rain gauge.

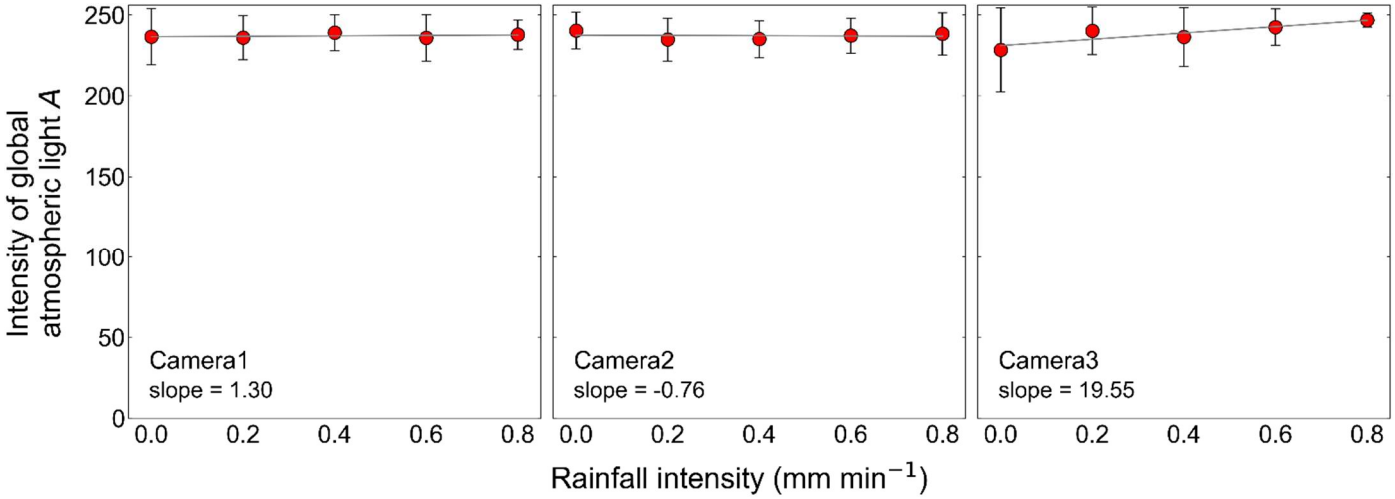


Figure 6. Distribution of global atmospheric light *A* by rainfall intensity. Each figure is marked with a camera name and slope of the linear regression line for the relationship between rainfall intensity and global atmospheric light *A*. The left figure is Camera 1, the center figure is Camera 2, and the right figure is Camera 3. The plots and error bars show the mean value and standard deviation of all data during the observation period. The straight lines show linear regression line for the relationship between rainfall intensity and global atmospheric light *A*. Rainfall intensity is observed by the rain gauge.

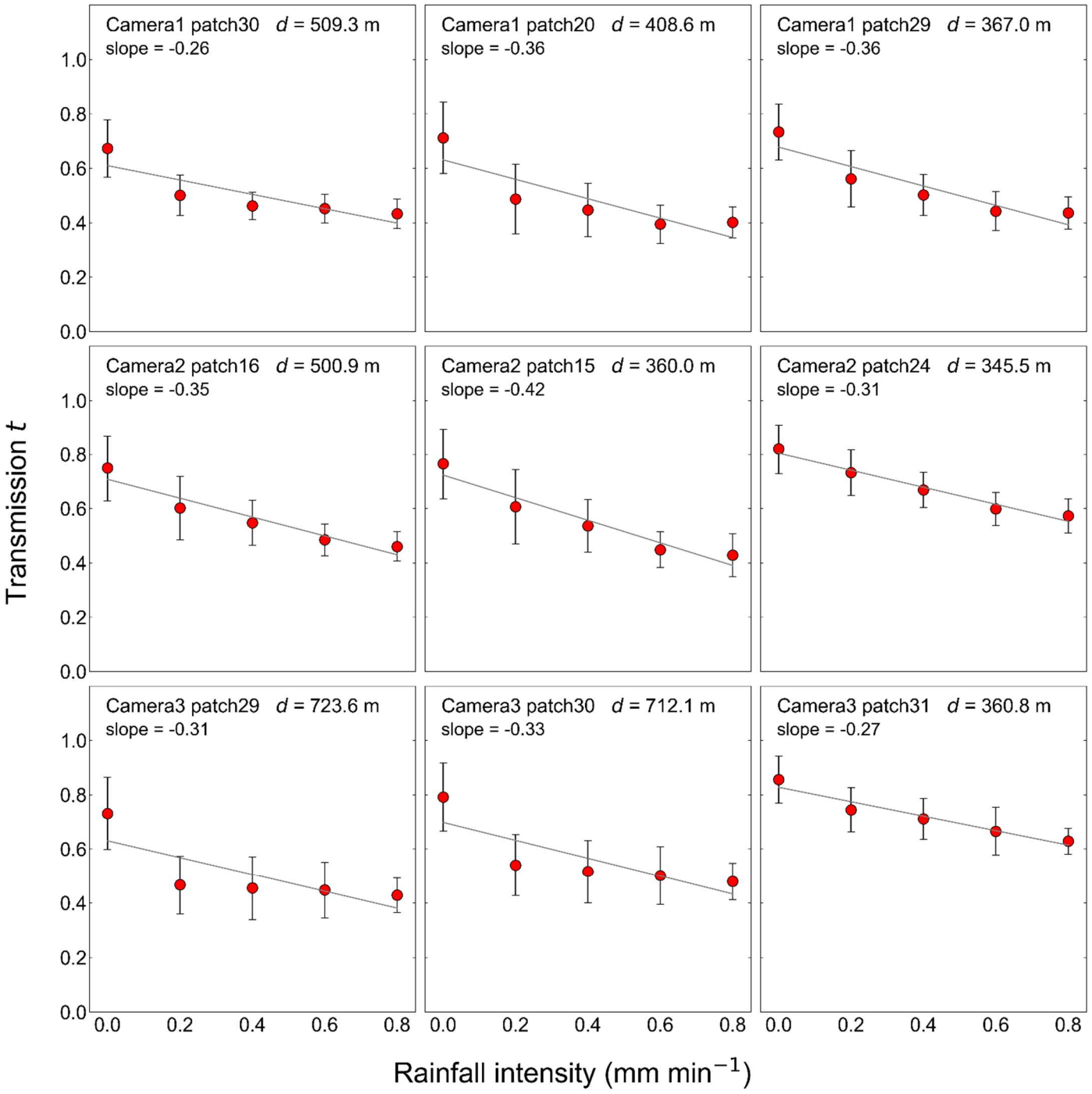


Figure 7. Distribution of transmission *t* by rainfall intensity. Figures show the top three patches of scene depth for each camera. Figures which include all patches are shown in Appendix C-3. Each figure is marked with a camera name, patch number, scene depth and slope of the linear regression line for the relationship between rainfall intensity and transmission *t*. The upper three figures are Camera 1, the middle three figures are Camera 2, and the lower three figures are Camera 3. The plots and error bars show the mean value and standard deviation of all data during the observation period. The straight lines show linear regression line for the relationship between rainfall intensity and transmission *t*. Rainfall intensity is observed by the rain gauge.

Appendix C-1: Figures including all patches showing the distribution of observed intensity *I* by rainfall intensity. Figure C-1-a, Figure C-1-b and Figure C-1-c show the distribution of observed intensity *I* by rainfall intensity of Camera 1, Camera 2 and Camera 3, respectively. Each figure is marked with a camera name, patch number, scene depth and slope of the linear regression line for the relationship between rainfall intensity and observed intensity *I*. The plots and error bars show the mean value and standard deviation of all data during the observation period. The straight lines show linear regression line for the relationship between rainfall intensity and observed intensity *I*. Rainfall intensity is observed by the rain gauge. Patches hatched in gray are patches where the appropriate scene depth could not be obtained due to the presence of sky background and the application of geometric corrections in the image registration process.

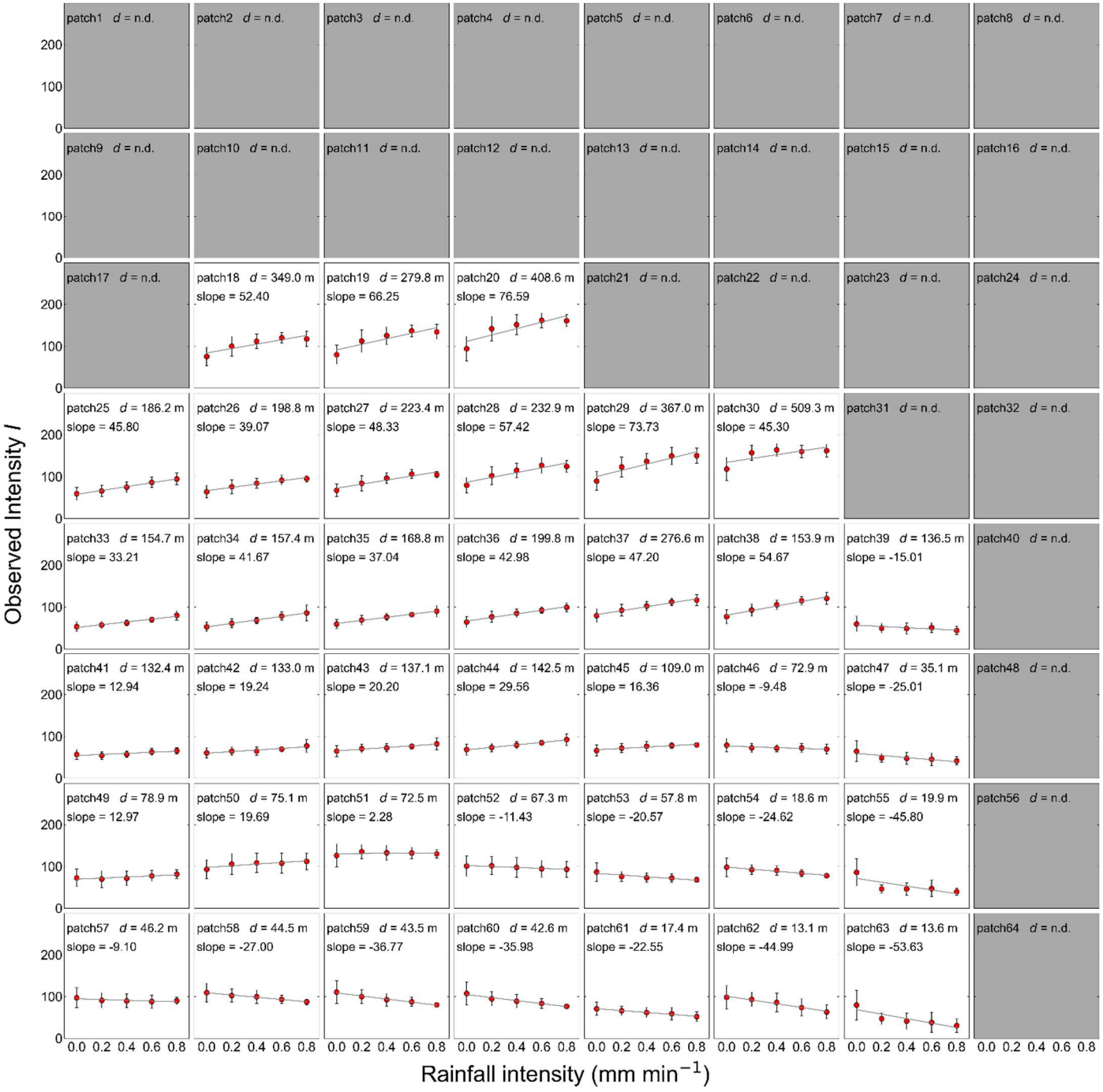


Figure C-1-a. Distribution of observed intensity *I* by rainfall intensity of Camera 1.

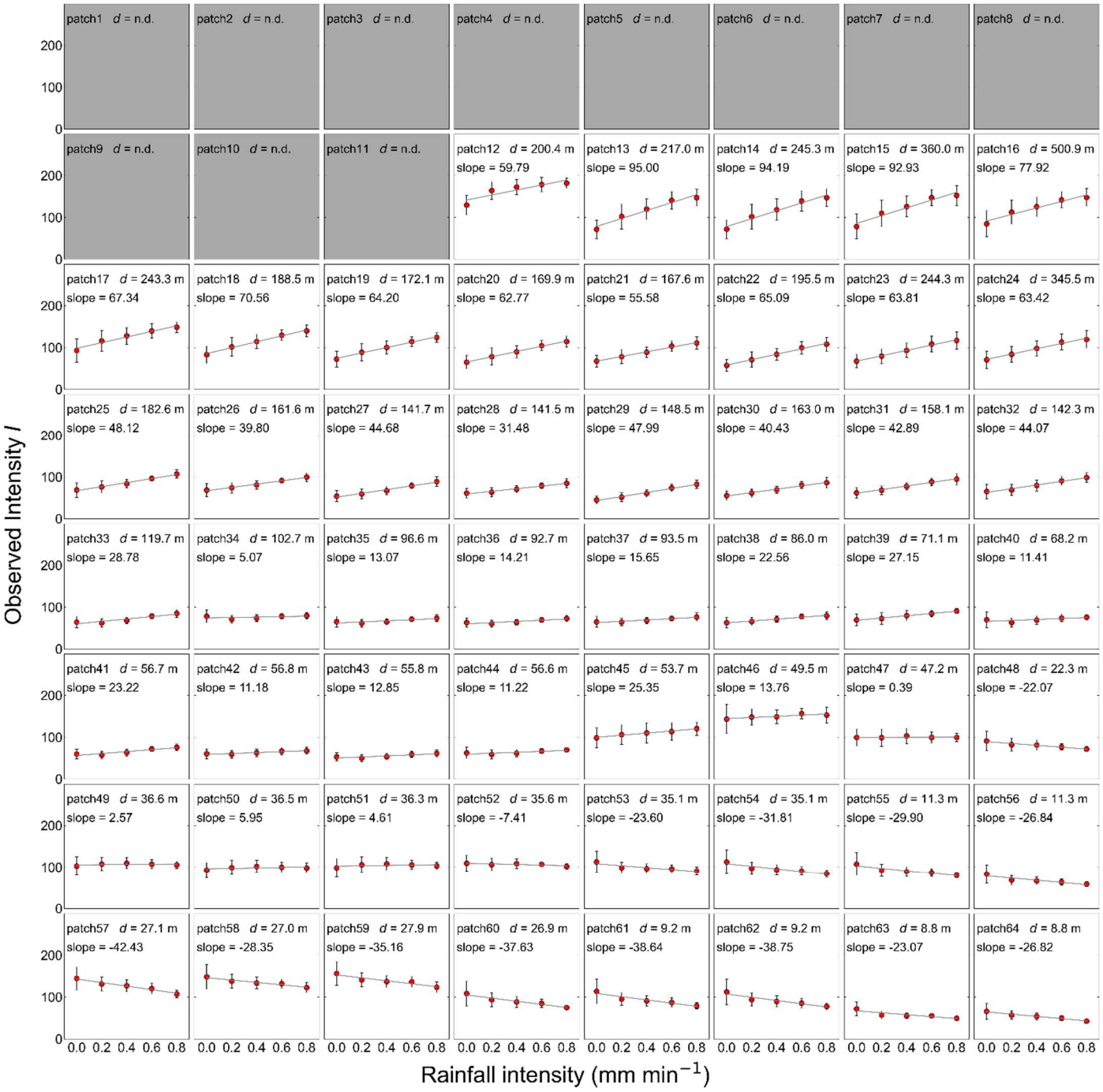


Figure C-1-b. Distribution of observed intensity *I* by rainfall intensity of Camera 2.

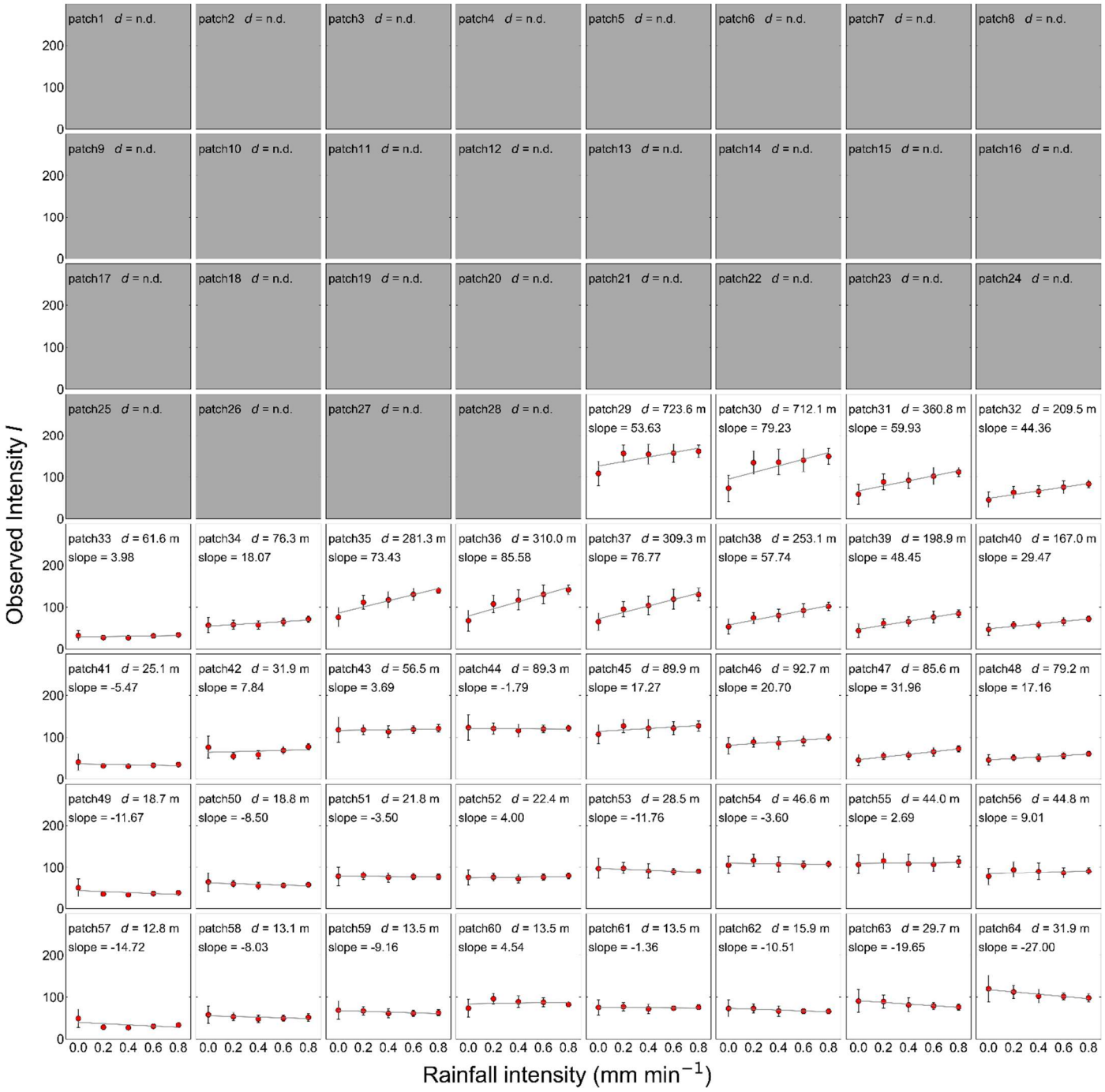


Figure C-1-c. Distribution of observed intensity *I* by rainfall intensity of Camera 3.

Appendix C-2: Figures including all patches showing the distribution of scene radiance *J* by rainfall intensity. Figure C-2-a, Figure C-2-b and Figure C-2-c show the distribution of scene radiance *J* by rainfall intensity of Camera 1, Camera 2 and Camera 3, respectively. Each figure is marked with a camera name, patch number, scene depth and slope of the linear regression line for the relationship between rainfall intensity and scene radiance *J*. The plots and error bars show the mean value and standard deviation of all data during the observation period. The straight lines show linear regression line for the relationship between rainfall intensity and scene radiance *J*. Rainfall intensity is observed by the rain gauge. Patches hatched in gray are patches where the appropriate scene depth could not be obtained due to the presence of sky background and the application of geometric corrections in the image registration process.

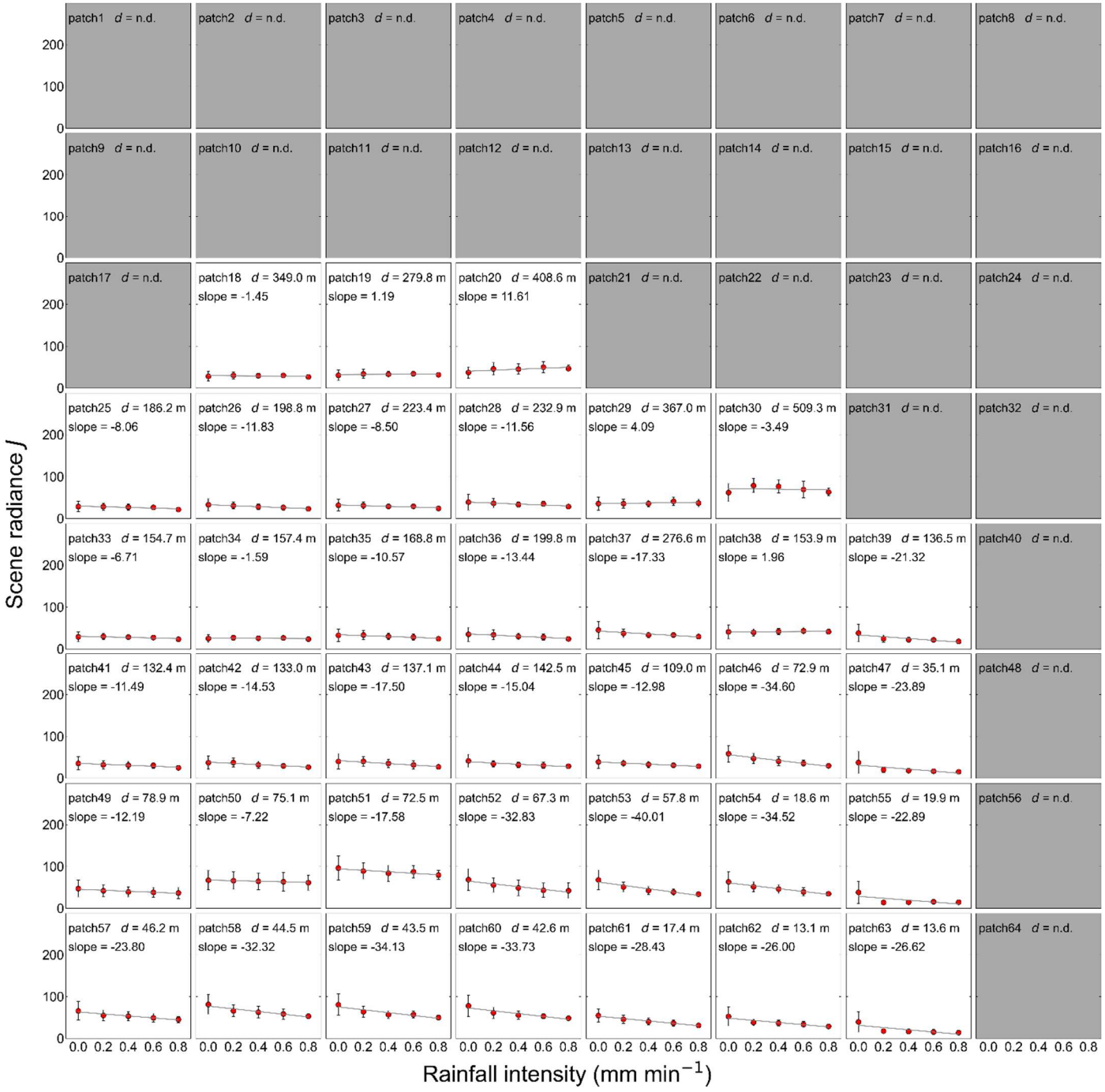


Figure C-2-a. Distribution of scene radiance *J* by rainfall intensity of Camera 1.

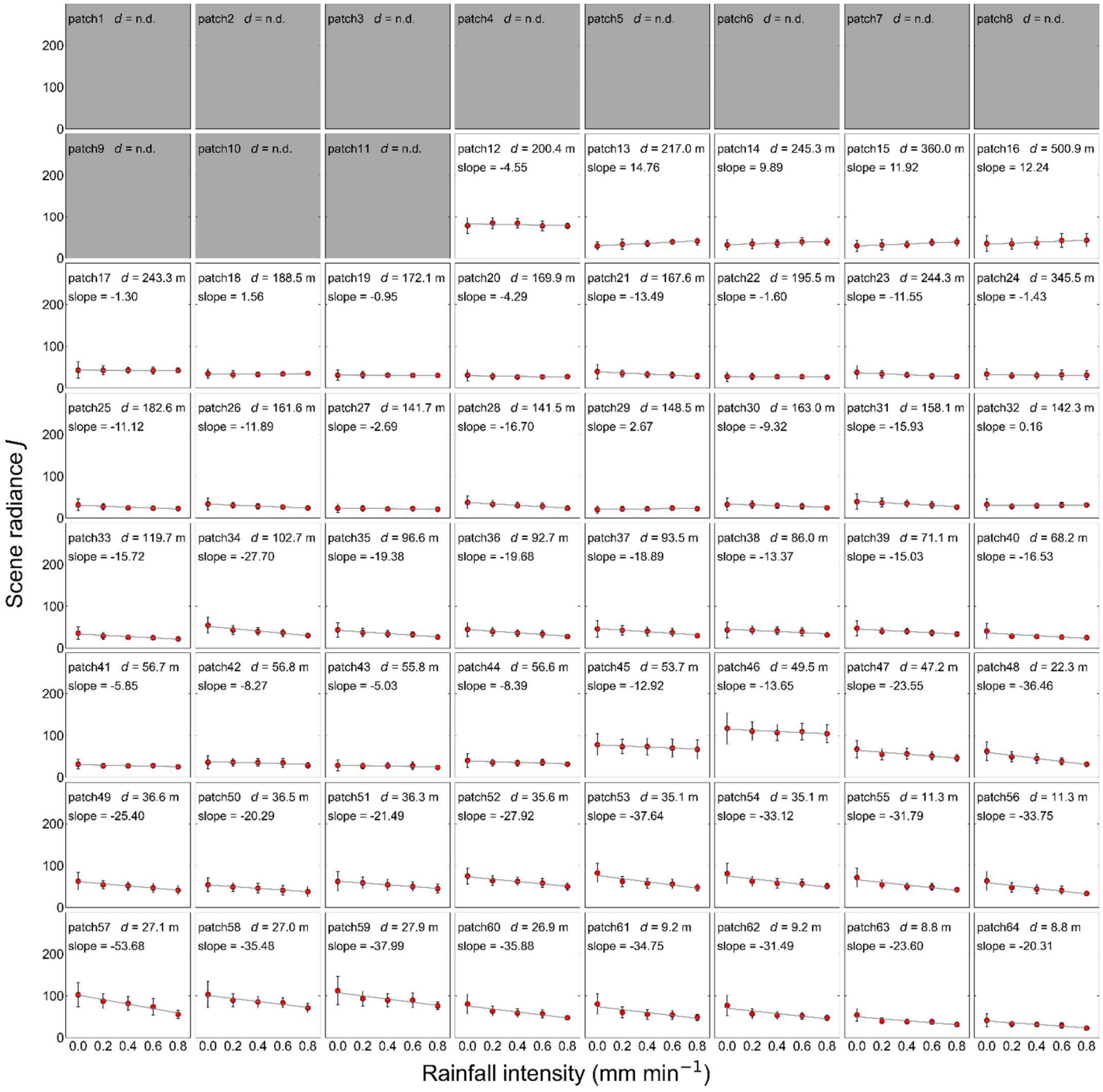


Figure C-2-b. Distribution of scene radiance *J* by rainfall intensity of Camera 2.

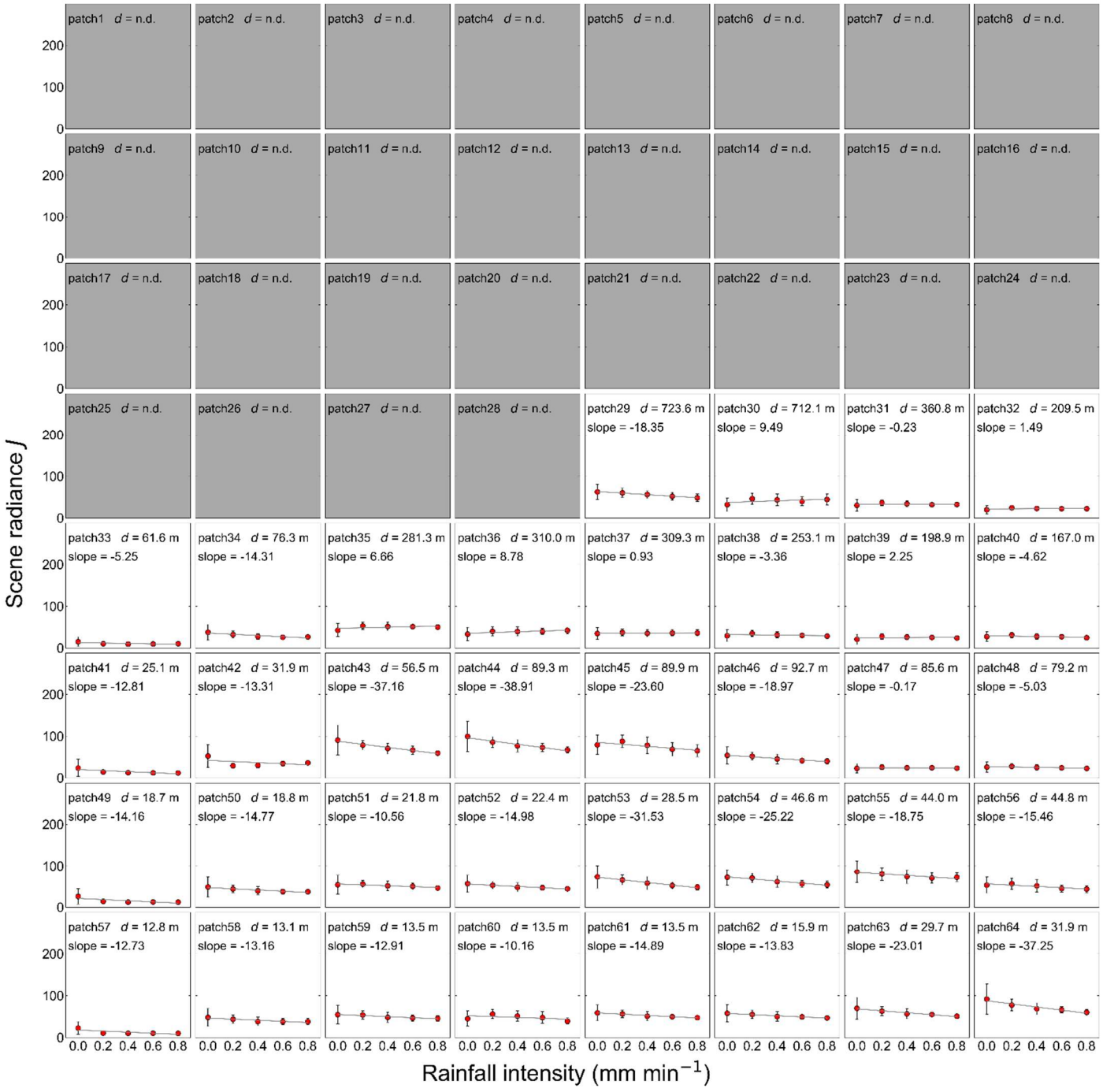


Figure C-2-c. Distribution of scene radiance *J* by rainfall intensity of Camera 3.

Appendix C-3: Figures including all patches showing the distribution of transmission *t* by rainfall intensity. Figure C-3-a, Figure C-3-b and Figure C-3-c show the distribution of transmission *t* by rainfall intensity of Camera 1, Camera 2 and Camera 3, respectively. Each figure is marked with a camera name, patch number, scene depth and slope of the linear regression line for the relationship between rainfall intensity and transmission *t*. The plots and error bars show the mean value and standard deviation of all data during the observation period. The straight lines show linear regression line for the relationship between rainfall intensity and transmission *t*. Rainfall intensity is observed by the rain gauge. Patches hatched in gray are patches where the appropriate scene depth could not be obtained due to the presence of sky background and the application of geometric corrections in the image registration process.

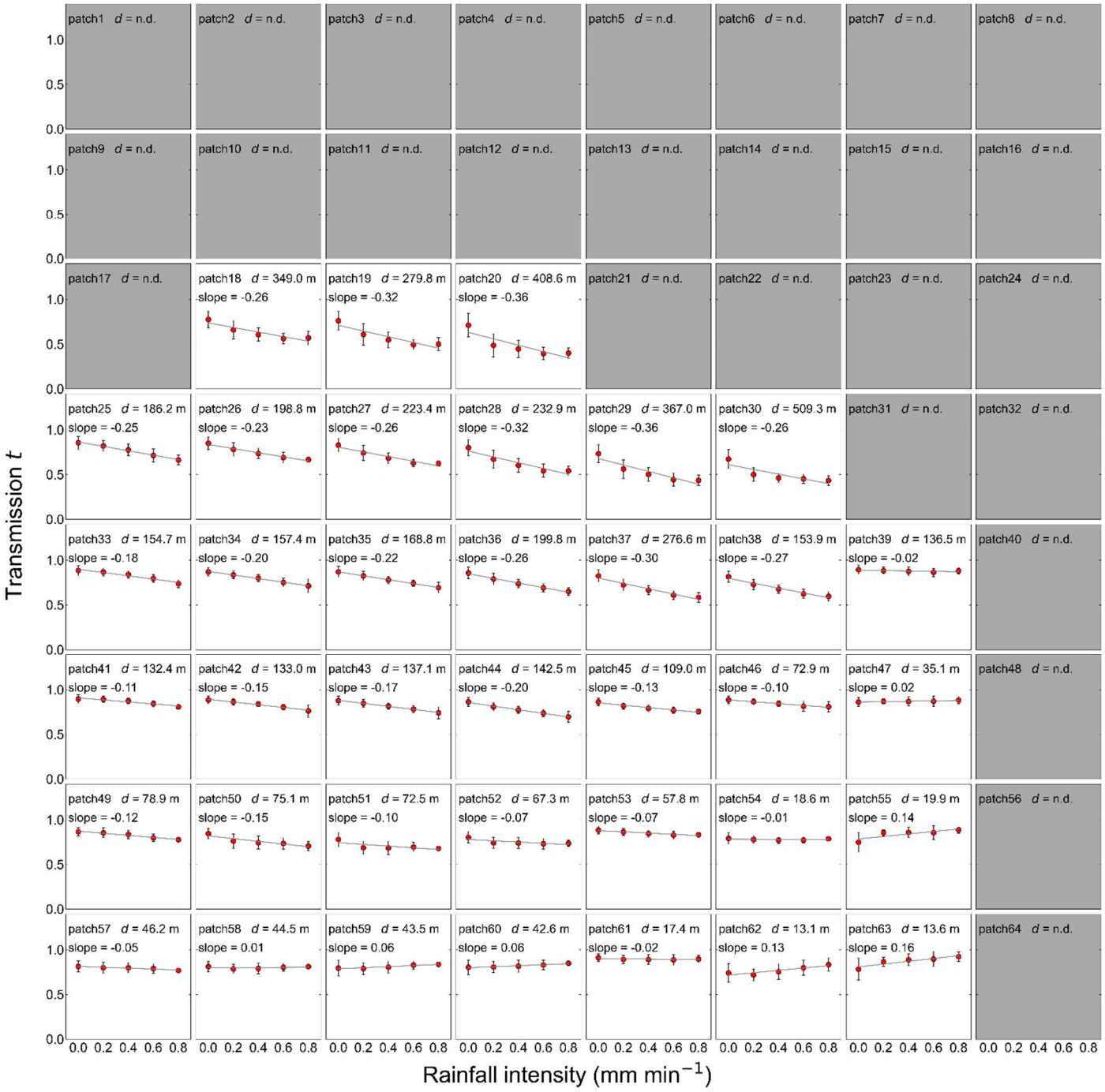


Figure C-3-a. Distribution of transmission *t* by rainfall intensity of Camera 1.

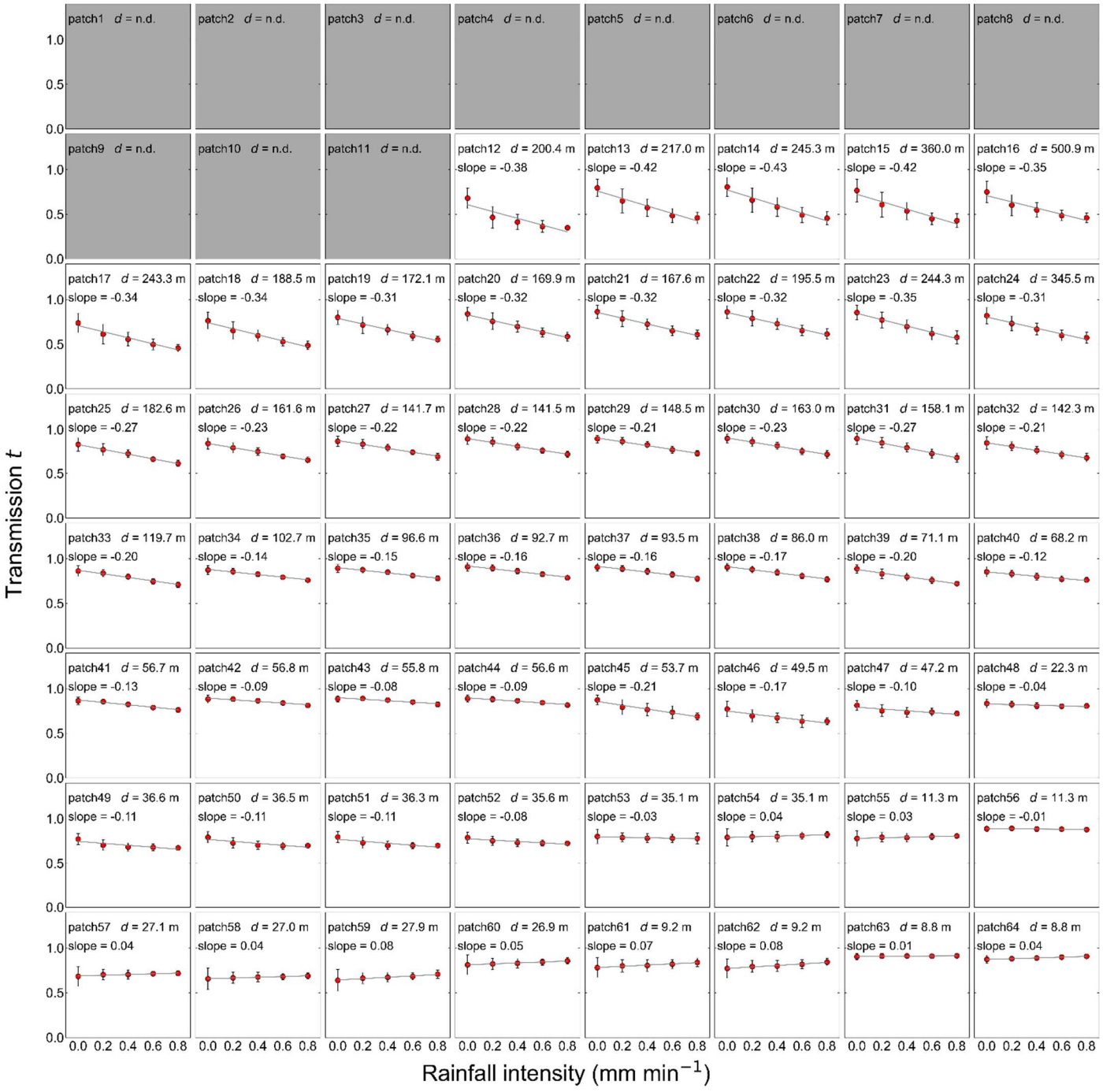


Figure C-3-b. Distribution of transmission *t* by rainfall intensity of Camera 2.

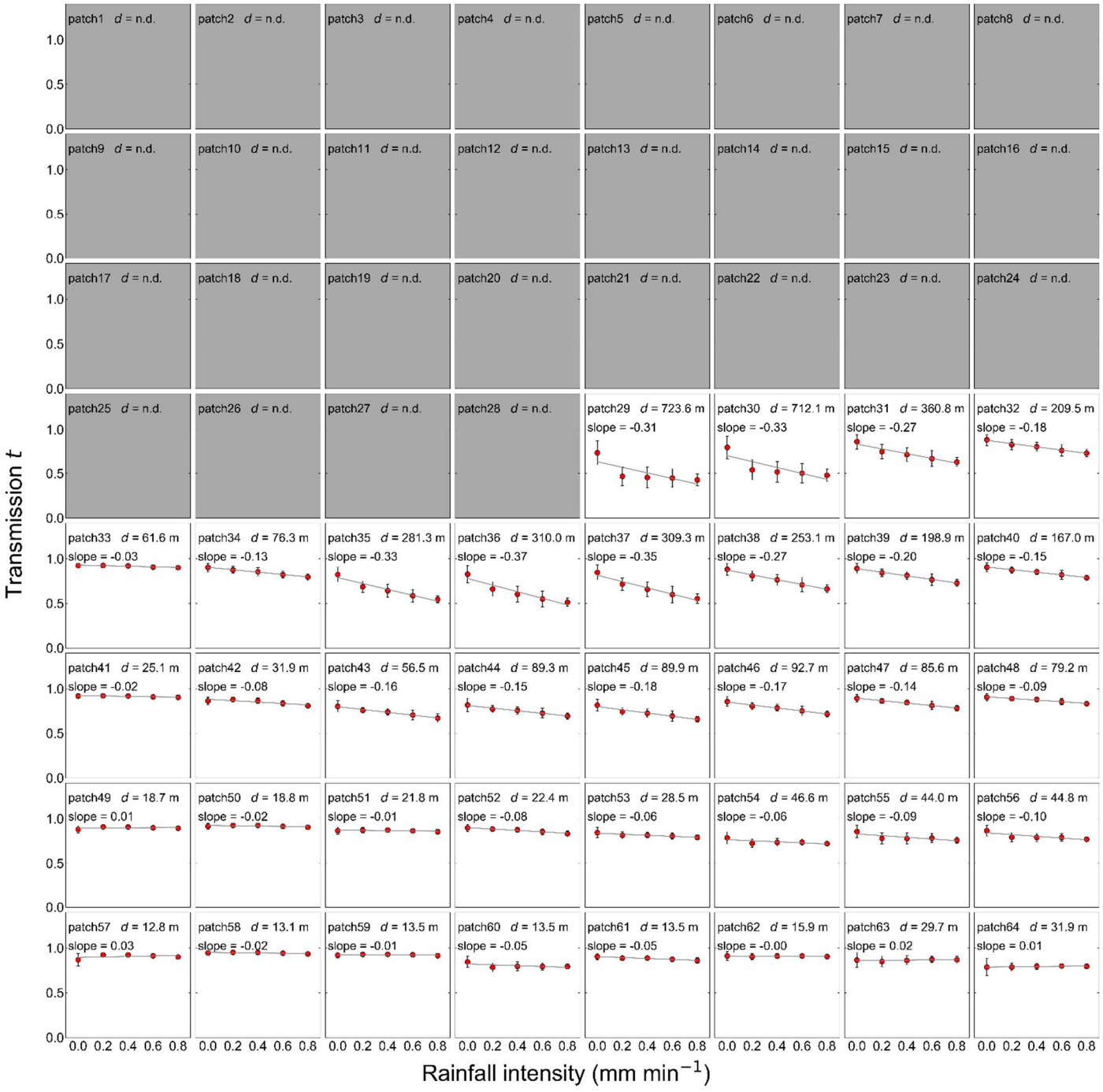


Figure C-3-c. Distribution of transmission *t* by rainfall intensity of Camera 3.

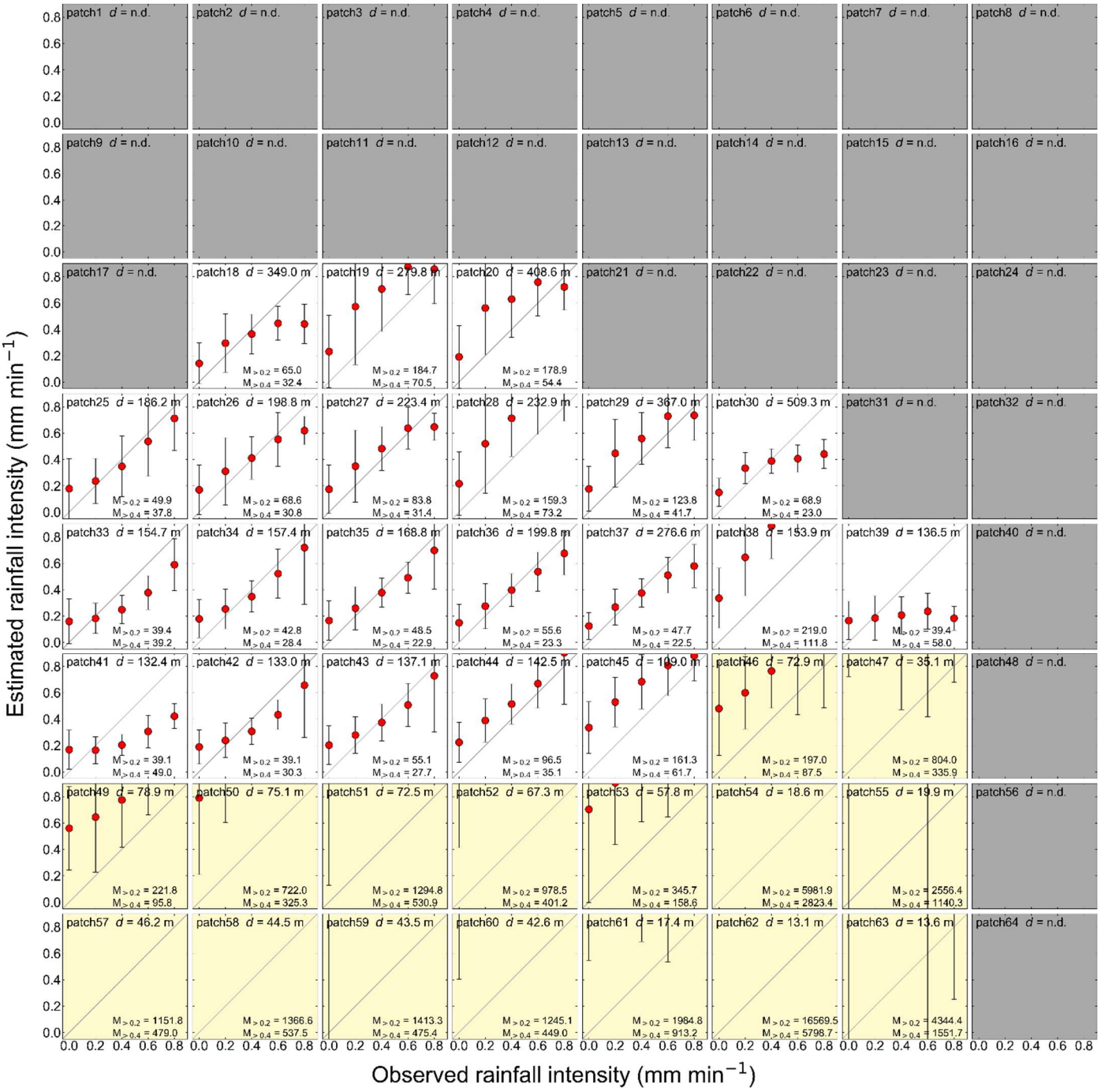


Figure 11-a. Relationship between observed rainfall intensity and estimated rainfall intensity of Camera 1. Each figure is marked with a patch number, scene depth and two MAPE values of rainfall intensity estimates throughout the observation period. $M_{>0.2}$ means MAPE value in cases using data with observed rainfall intensity of 0.2 mm min$^{-1}$ or greater and $M_{>0.4}$ means MAPE value in cases using data with observed rainfall intensity of 0.4 mm min$^{-1}$ or greater. The plots and error bars show the mean value and standard deviation of all data during the observation period. Patches hatched in yellow indicate patches with scene depth of less than 100 m. Patches hatched in gray are patches where the appropriate scene depth could not be obtained due to the presence of sky background and the application of geometric corrections in the image registration process.

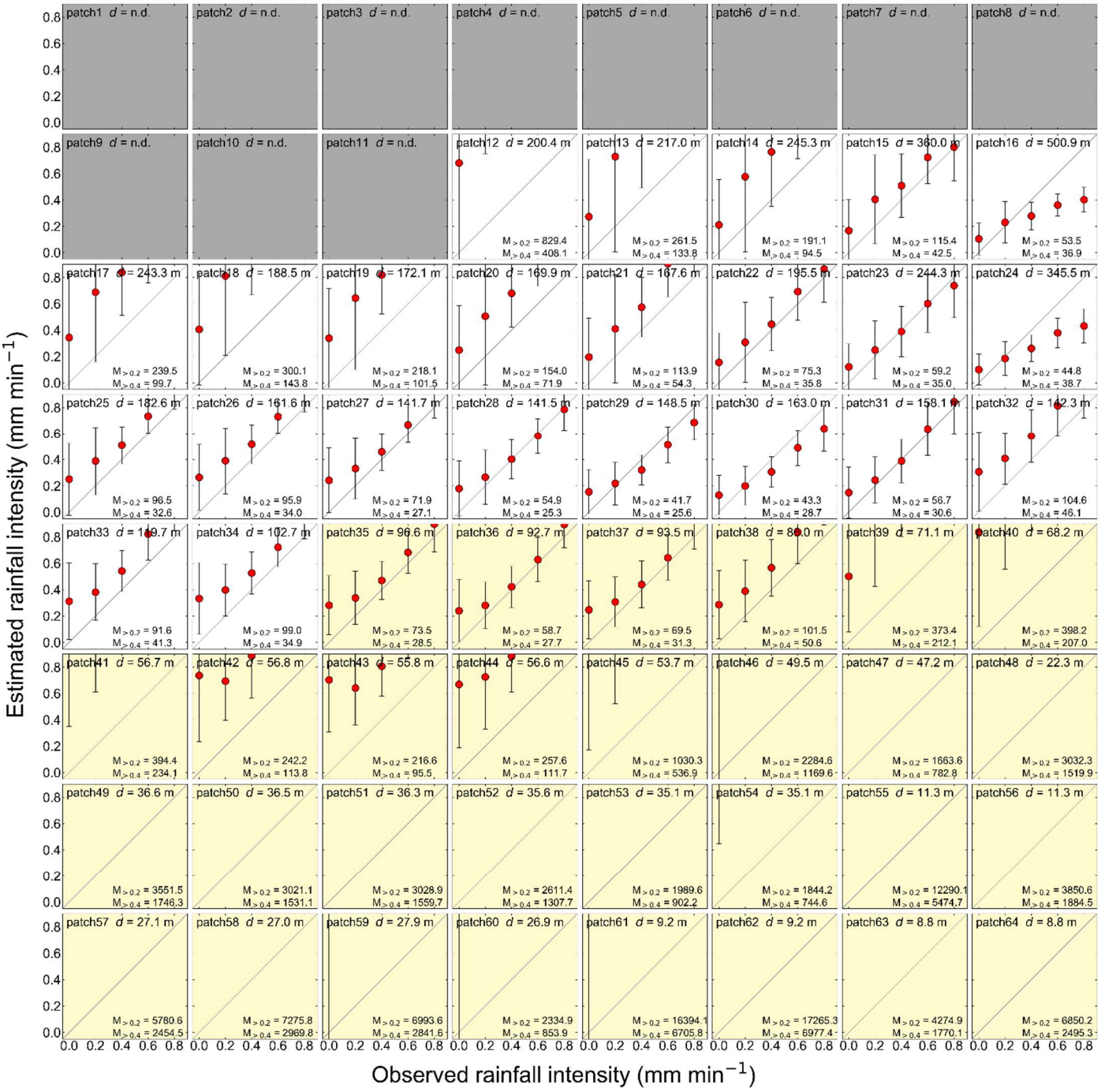


Figure 11-b. Relationship between observed rainfall intensity and estimated rainfall intensity of Camera 2. Each figure is marked with a patch number, scene depth and two MAPE values of rainfall intensity estimates throughout the observation period. $M_{>0.2}$ means MAPE value in cases using data with observed rainfall intensity of 0.2 mm min$^{-1}$ or greater and $M_{>0.4}$ means MAPE value in cases using data with observed rainfall intensity of 0.4 mm min$^{-1}$ or greater. The plots and error bars show the mean value and standard deviation of all data during the observation period. Patches hatched in yellow indicate patches with scene depth of less than 100 m. Patches hatched in gray are patches where the appropriate scene depth could not be obtained due to the presence of sky background and the application of geometric corrections in the image registration process.

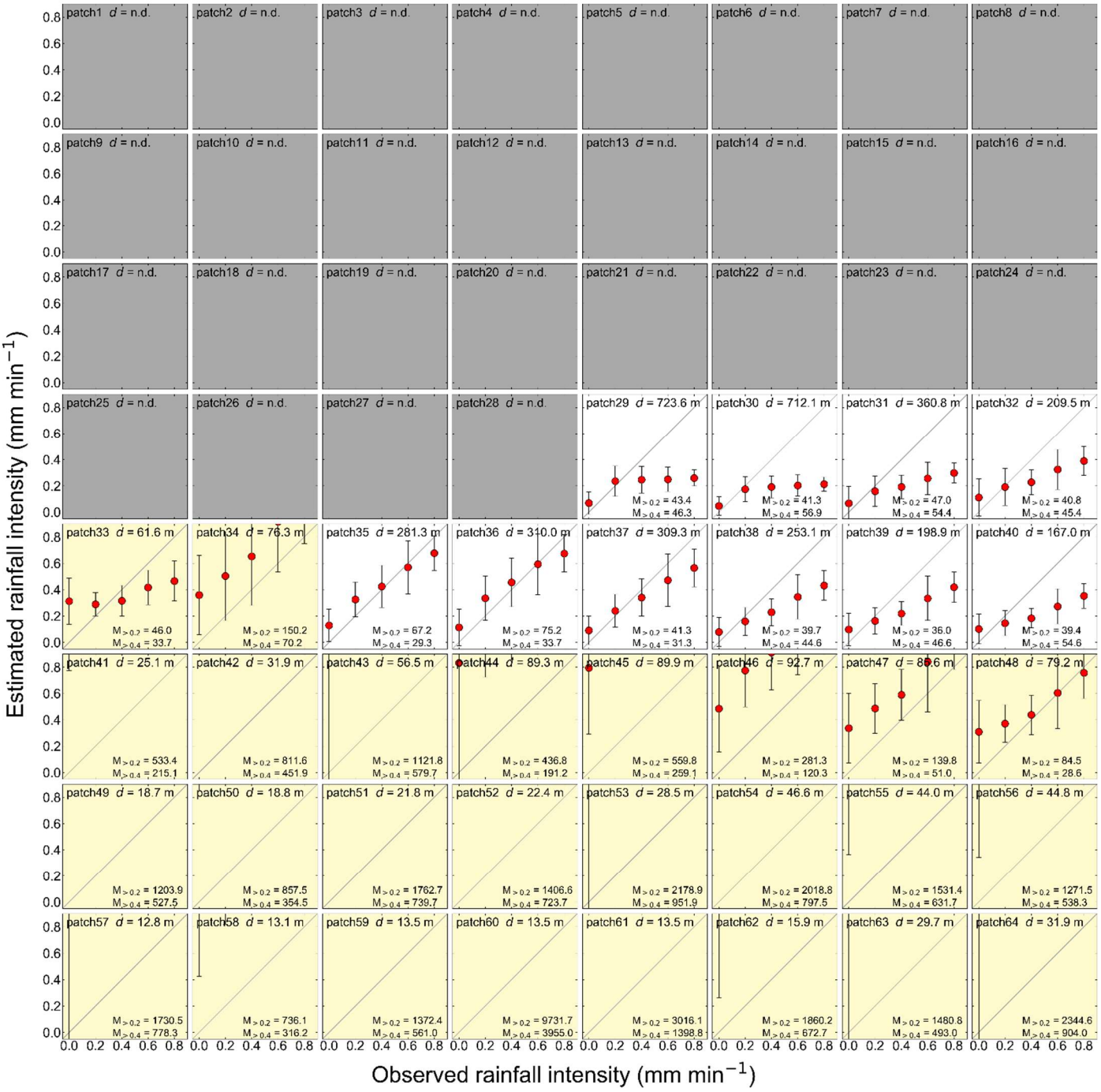


Figure 11-c. Relationship between observed rainfall intensity and estimated rainfall intensity of Camera 3. Each figure is marked with a patch number, scene depth and two MAPE values of rainfall intensity estimates throughout the observation period. $M_{>0.2}$ means MAPE value in cases using data with observed rainfall intensity of 0.2 mm min$^{-1}$ or greater and $M_{>0.4}$ means MAPE value in cases using data with observed rainfall intensity of 0.4 mm min$^{-1}$ or greater. The plots and error bars show the mean value and standard deviation of all data during the observation period. Patches hatched in yellow indicate patches with scene depth of less than 100 m. Patches hatched in gray are patches where the appropriate scene depth could not be obtained due to the presence of sky background and the application of geometric corrections in the image registration process.

**< Comment 3 >**

- The experiment has been conducted at outdoor sitting using three commercial camera, which are the brand type and specifications of each camera separately (country of origin and description number of the device) such as “the UV visible spectrophotometer (model T80 × UVNIS Spectrometer PG Instruments Ltd, England)”. This must be included in the material section. And what is the camera's shooting range (km)?

Response:

We will revise L.203 through 204 as follows.

“Photography was taken using three commercially available interval cameras (TLC200Pro Brinno inc., Taiwan).”

We consider shooting range and focus distance to mean almost the same thing and it is from 40 cm to infinity as shown L. 206.

We will also revise L. 215 to have the same description about a tipping bucket rain gauge used as follows.

“One-minute rainfall intensity was also observed using a tipping bucket rain gauge (RG3-M Onset Computer Corporation, USA) at almost the same locations where the cameras were installed.”

**< Comment 4 >**

- Details about the monthly meteorological data (wind speed, relative humidity, max and min temperature) for the experiment period are missing. Please describe it in figure…

Response:

We will add the following figure and text in L. 203.

“The meteorological observations in 2021 around the observation site are shown in Figure **. The figure shows data from a weather station about 24 km southeast of those cameras. The Köppen climate classification of the area around the observation site is humid subtropical climate, with hot, humid and heavy precipitation in summer and cool to mild in winter.”

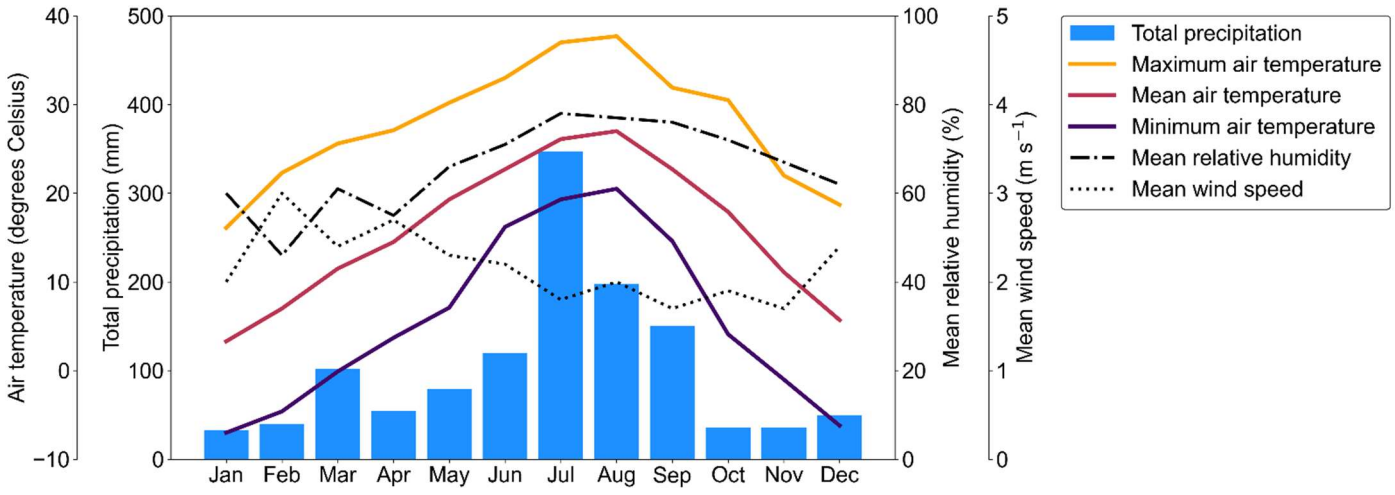


Figure **. The meteorological observations in 2021 around the observation site.

**< Comment 5 >**

- As for the figures (4,5,7) and the table (2), there is very dense data in them. Please simplify the presentation of the results in a way that makes it easy for the reader to understand and grasp the information easily and without feeling any distraction.

Response:

As shown in our response to Comment 2, we will revise Figures 4, 5, and 7. The revised Figures 4, 5, and 7 show the top three

patches of scene depth for each camera. In terms of Figures 4, 5, and 7, we will move Figures which include all patches to an appendix C-1, C-2, and C-3. Furthermore, we will remove Table. 2 and add the information in Table 2 to Figure 4, 5, and 7. We will also revise Figure 6 to have the same appearance as shown in our response to Comment 2.

**< Comment 6 >**

- As for the results section... it shows very valuable and very important results, so it needs to be written in more detail and more clarity.

Response:

We will revise the results section 4.1 as follows. As shown in response to Comment 5, we will revise Figures 4 ,5 ,6 and 7 for better clarity.

"4.1 Distribution of observed intensity *I*, scene radiance *J*, global atmospheric light *A*, and transmission *t*

Figures 4, 5, and 7 show the distribution of observed intensity *I*, scene radiance *J*, and transmission *t* for each rainfall intensity, respectively. These figures show the top three patches of scene depth for each camera. This is because the greater the scene depth, the more likely static weather effects are to appear, making it easier to understand the characteristics of static weather effects. Figures which include all patches are shown in Appendix C-1, C-2, and C-3. Figures 6 show the distribution of global atmospheric light *A* for each rainfall intensity. Global atmospheric light *A* is set to one value per image, regardless of the patch. Furthermore, the slope of the regression line by single regression analysis in the relationship between rainfall intensity and the mean values of observed intensity *I*, scene radiance *J*, global atmospheric light *A*, and transmission *t* are shown in Figures 4, 5, 6, and 7. Although an exponential relationship between rainfall intensity and observed intensity *I*, scene radiance *J*, global atmospheric light *A*, and transmission *t* is expected as shown in Eqs. (7) and (8), a simple regression analysis was conducted here to analyze a simple trend.

As shown in Figure 4, the mean values of observed intensity *I* range from approximately 50 to 200, and the value and distribution range of observed intensity *I* vary for each patch. For example, comparing the figures for patches 30 and 29 of camera 1 in the upper panel of Figure 4, when the rainfall intensity is 0.0 mm $min^{-1}$, the mean value of observed intensity *I* in patch 30 is approximately 120, while in patch 29, it is approximately 90. Similarly for the other cameras, each patch has a different observed intensity when the rainfall intensity is 0.0 mm $min^{-1}$. This is because the background color and luminance are inherently different due to the different background objects in each patch. On the other hand, the tendency of increasing observed intensity *I* as the rainfall intensity increases is consistent across all patches although the slope of the regression line is different in each patch somewhat. This means that, as an overall trend, the whiteness of the image increases as rainfall intensity increases. Furthermore, in patches with particularly large scene depths, such as patch 30 of Camera 1, patch 29 of Camera 3, and patch 30 of Camera 3, observed intensity *I* tend to increase significantly when the rainfall intensity is 0.2 mm $min^{-1}$, and then remains almost constant even if the rainfall intensity increases further. This suggests that there is an upper limit to the observed intensity *I*, and that scene depth and rainfall intensity may interrelate to determine the extent of increase in observed intensity *I*.

Next, as shown in Figure 5, the mean values of scene radiance *J* range from approximately 0 to 100. The tendency of scene radiance *J* is different from the tendency of observed intensity *I*, and the effect of rainfall intensity is limited and varies little in any of the cameras. Moreover, as shown in Figure 6, the mean values of global atmospheric light *A* range from approximately 200 to 250, and the effect of rainfall intensity on global atmospheric light *A* is also limited and varies little in any of the cameras.

Finally, as shown in Figure 7, the mean values of transmission *t* range from approximately 0.4 to 1, and the value and distribution range of transmission *t* vary for each patch. On the other hand, the tendency of decreasing transmission *t* as

the rainfall intensity increases is consistent across all patches and is opposite to the tendency of the relationship between observed intensity $I$ and rainfall intensity. This tendency between transmission $t$ and rainfall intensity quantitatively indicates that the background becomes gradually hazy and less visible as the rainfall intensity increases. Furthermore, in patches with particularly large scene depths, such as patch 30 of Camera 1, patch 29 of Camera 3, and patch 30 of Camera 3, transmission $t$ tends to decrease significantly when the rainfall intensity is 0.2 mm $min^{-1}$, and then remains almost constant even if the rainfall intensity increases further. As with the case of observed intensity $I$, this suggests that there is a lower limit to the transmission $t$, and that scene depth and rainfall intensity may interrelate to determine the extent of decrease in transmission $t$."

In addition, we will add the following sentence in L.325.

"As described in 4.1, the fact that scene depth and rainfall intensity may interrelate to determine the extent of decrease in transmission $t$ is also in the same sense."

**< Comment 7 >**

- The discussion section needs work. There are no comparisons with other studies. The discussion section must be rewritten in-depth highlighting the limitations of the present study.

Response:

In terms of the validity of calculated extinction coefficient $\beta$, we compared our results to other studies as shown in 5. 2. 3, and 5. 2. 4. Furthermore, in terms of the accuracy of estimated rainfall intensity, we compared our results to other previous studies as shown in Table 4. We will revise Table 4 as follows. The revised Table 4 shows mean, maximum, 75 percentile, median, 25 percentile and minimum values of MAPE over all patches and patches with scene depth of more than 100 m.

Table 4. Comparison of accuracy between five previous studies and this study: The "City, Country" row indicates the city and country where each study was conducted, and the "Köppen climate classification" row indicates the Köppen climate classification of the city. In the "Used data" row, "> 0.2 mm min-1" means that data with observed rainfall intensity of 0.2 mm min-1 or greater were used, and "> 0.4 mm min-1" means that data with observed rainfall intensity of 0.4 mm min-1 or greater were used. The "Observed rainfall intensity" row indicates the mean, maximum and minimum rainfall intensity during the observation period for each study. The range of "Observed rainfall intensity" indicates the range due to multiple rainfall events in each study. The rainfall intensity of Jiang et al. (2019) was converted from the duration and the accumulated rainfall of the rainfall event. MAPE is the mean absolute percentage error, and data with observed rainfall intensity of 0 mm min-1 were excluded by the definition of MAPE. MAPE values are shown for the case where all patches were used and for the case where only patches with a scene depth of more than 100 m were used. The number of patches used for each camera is shown in parentheses. In the column of the minimum MAPE, the patch number indicating the minimum value is shown in parentheses.

| | | | This study | | | | | | Allamano et al. (2015) | Dong et al. (2017) | Jiang et al. (2019) | Yin et al. (2023) | Zheng et al. (2023) |
|---|---|---|---|---|---|---|---|---|---|---|---|---|---|
| City, Country | | | Yamanashi, Japan | | | | | | Torino, Italy | Nanjing, China | Shenzhen, China | Hangzhou, China | Hangzhou, China |
| Köppen climate classification | | | Humid subtropical climate (Cfa) | | | | | | Humid subtropical climate (Cfa) | Humid subtropical climate (Cfa) | Monsoon influenced humid subtropical climate (Cwa) | Humid subtropical climate (Cfa) | Humid subtropical climate (Cfa) |
| Used data | | | > 0.2 mm min$^{-1}$ | | | > 0.4 mm min$^{-1}$ | | | - | - | - | - | - |
| Camera name | | | Camera 1 | Camera 2 | Camera 3 | Camera 1 | Camera 2 | Camera 3 | - | - | - | - | - |
| Data size for validation: Video length (min) | | | 3261 | 3015 | 3261 | 120 | 107 | 120 | 104 | 9 | 403 | 170 | 357 |
| Observed rainfall intensity (mm h$^{-1}$) | | Mean | 12.6 | 12.6 | 12.6 | 28.5 | 28.9 | 28.5 | 2.8 - 9.3 | 1.1 - 6.5 | 4.1 - 29.5 | 11.0 - 23.6 | 9.7 - 39.3 |
| | | Maximum | 48.0 | 48.0 | 48.0 | 48.0 | 48.0 | 48.0 | 6.0 - 38.2 | - | - | 36.0 - 66.0 | 24.0 -156.0 |
| | | Minimum | 12.0 | 12.0 | 12.0 | 24.0 | 24.0 | 24.0 | 1.3 - 3.2 | - | - | - | - |
| Accuracy: MAPE (%) | All patches (Camera 1: 37 patches, Camera 2: 53 patches, Camera 3: 36 patches) | Mean | 1163.4 | 2131.4 | 1087.2 | 459.7 | 923.8 | 466.3 | 26.0 | 31.8 | 21.8 | 13.5 - 21.9 | 10.4 - 18.0 |
| | | Maximum | 5981.9 | 12290.1 | 2178.9 | 2823.4 | 5474.7 | 951.9 | | | | | |
| | | 75 percentile | 783.5 | 1989.6 | 1296.7 | 333.2 | 853.9 | 565.7 | | | | | |
| | | Median | 170.1 | 242.2 | 546.6 | 66.1 | 111.7 | 237.1 | | | | | |
| | | 25 percentile | 55.6 | 95.9 | 62.2 | 32.4 | 36.9 | 49.9 | | | | | |
| | | Minimum | 39.1 (patch 42) | 41.7 (patch 29) | 36.0 (patch 39) | 22.5 (patch 37) | 25.3 (patch 28) | 28.6 (patch 48) | | | | | |
| | Patches with scene depth of more than 100 m (Camera 1: 21 patches, Camera 2: 23 patches, Camera 3: 10 patches) | Mean | 88.9 | 148.3 | 47.1 | 43.1 | 70.6 | 44.3 | | | | | |
| | | Maximum | 219.0 | 829.4 | 75.2 | 111.8 | 408.1 | 56.9 | | | | | |
| | | 75 percentile | 123.8 | 172.5 | 46.1 | 54.4 | 83.2 | 52.5 | | | | | |
| | | Median | 65.0 | 96.5 | 41.3 | 35.1 | 38.7 | 45.9 | | | | | |
| | | 25 percentile | 47.7 | 58.0 | 40.0 | 28.4 | 33.3 | 36.4 | | | | | |
| | | Minimum | 39.1 (patch 42) | 41.7 (patch 29) | 36.0 (patch 39) | 22.5 (patch 37) | 25.3 (patch 28) | 29.3 (patch 35) | | | | | |

The revised Table 4 shows the city and country where each study was conducted, the Köppen climate classification of the city, and the mean, maximum and minimum rainfall intensity during the observation period for each study. Table 4 shows that although only Jiang et al. (2019) was conducted in Monsoon influenced humid subtropical climate, this study and all five previous studies were conducted in a humid subtropical climate, and that there are no significant climatic differences. Furthermore, regarding the mean rainfall intensity during the observation period, the mean rainfall intensities of Allamano et al. (2015) and Dong et al. (2017) were lower than those in this study, while the mean rainfall intensities of Jiang et al. (2019), Yin et al. (2023), and Zheng et al. (2023) were comparable to this study. Overall, there is no significant difference in mean rainfall intensity between this study and the five previous studies. Moreover, in all studies, MAPE, a metrics of model performance, was calculated from observed values and model prediction. Given these facts, it seems reasonable to compare this study with five previous studies.

Therefore, we will add the following text in L. 603.

"Table 4 shows that although only Jiang et al. (2019) was conducted in Monsoon influenced humid subtropical climate, this

study and all five previous studies were conducted in a humid subtropical climate, and that there are no significant climatic differences. Furthermore, regarding the mean rainfall intensity during the observation period, the mean rainfall intensities of Allamano et al. (2015) and Dong et al. (2017) were slightly lower than those in this study, while the mean rainfall intensities of Jiang et al. (2019), Yin et al. (2023), and Zheng et al. (2023) were comparable to this study. Overall, there is no significant difference in mean rainfall intensity between this study and the five previous studies. Moreover, in all studies, MAPE, a metrics of model performance, was calculated from observed values and model prediction. Given these facts, it seems reasonable to compare this study with five previous studies."

In addition, we will rewrite the limitations of the present study in the discussion section as shown in our response to Comment 12.

**< Comment 8 >**

- The research is based on how commercial cameras are used to measure rainfall and the effect of this rainfall on the measurement accuracy of each type of camera separately.... But how can we overcome the problem of the inefficiency of commercial cameras in measuring rainfall with high accuracy... Can the efficiency of the camera be improved... What is the best type of the three camera ... How can we help stakeholders in manufacturing a high-resolution surveillance camera at a low price... Please explain this

Response:

It is certainly inefficient to install new cameras for rainfall observation. However, as shown in L. 105 through 106, the intention of this study is to efficiently use images from cameras already installed for other purposes to measure rainfall intensity. All three cameras used in this study are the same model. These cameras are commercially available for approximately 300 US dollars per unit and are relatively accessible to everyone.

**< Comment 9 >**

- How to solve the problem of commercial cameras deteriorating due to increased rainfall.... please explain

Response:

As shown in our response to Comment 1, we will revise the title because the original title was unclear. This study did not discuss camera performance degradation to increased rainfall.

**< Comment 10 >**

- Can farmers use a rainfall monitoring camera on their farmland to track rainfall and calculate irrigation rates efficiently.... Or will it be too expensive for them? Please clarify.

Response:

As shown in L. 672, this method requires only camera image taken of the background over a certain distance and background scene depth information. The camera we used is a commercial camera costing approximately 300 US dollars per unit and is not so expensive. Therefore, farmers can easily use those cameras and monitor rainfall.

**< Comment 11 >**

- The research compares types of commercial cameras... please clarify which categories can benefit most from these results and apply the research results on a practical and realworld scale.

Response:

As shown in L. 27 through 29, in mountainous areas where flash floods and debris flow occur, rainfall should be measured on fine spatial and temporal scales for effective early warning against these disasters. In such areas, even if rain gauges are not installed, monitoring cameras may be in place. This study attempts to observe rainfall by effectively utilizing such cameras already installed for other purposes. We expect that our research results can be applied on a practical and realworld scale in the category of disaster prevention.

Therefore, we will revise L. 681 through 684 as follows.

“Especially, in mountainous areas where flash floods and debris flow occur, for countermeasures against these disasters, it is desirable to have information on rainfall with high spatio-temporal resolution. In such areas, even if rain gauges are not installed, monitoring cameras may be in place. This study attempts to observe rainfall by effectively utilizing such cameras already installed for other purposes. We expect that our research results can be applied on a practical and realworld scale in such category of disaster prevention.”

**< Comment 12 >**

- Please clarify at the end of the discussion section what are the weaknesses and future studies that should be conducted for improvement and to reach the best results that help in solving problems related to hydrology and rainfall.

Response:

We will remove L. 611 through 626, and add a new discussion section “5. 4 Ways of forwards” as follows to clearly show the weaknesses and future studies that should be conducted for improvement. Furthermore, we will add related paper to references.

“5. 4 Ways forwards

5. 4 .1 Limitation of the proposed method

There are still several technical problems that need to be solved in the method of this study. The first problem is how to select an appropriate background for rainfall intensity estimation (i.e., the analysis area to be used for rainfall intensity estimation). As shown in Table 4, the accuracy of rainfall intensity estimation varies greatly depending on the background patch selected. Therefore, background patches with the highest estimation accuracy possible should be selected. One solution to this problem is to select patches with a scene depth of more than 100 m . As shown in Table 4, selecting analysis regions from patches with scene depth of more than 100 m is more accurate overall than selecting analysis regions from all background patches. On the other hand, it may also be important that the scene depth is not too large because even relatively small rainfall intensity may cause the transmission to reach the lower limit as shown in Figure 7. It is necessary to further study in detail what scene depth is appropriate for rainfall intensity estimation. In addition, in terms of background objects, a relatively undisturbed background is desirable for the analysis area. Therefore, it is preferable to choose a static background such as building walls, tree canopies, and ground surface without people or vehicles, especially when applying this method in urban areas. However, at this time, the selection of appropriate backgrounds has not been analyzed in detail, and further study is needed on the effects of scene depth, background texture, and dynamic subject exposure on estimation accuracy.

The second problem is how to remove the effects of dew formation and raindrops on the camera lens itself from the image. Dew formation and raindrops on the camera lens itself could cause significant blurring of the image and affect the rainfall estimation results, but this effect has not been analyzed at this time. Therefore, it is necessary to consider how to physically protect the camera lens (e.g., by covering the camera with a cover) and how to remove the effect from the image

if dew or raindrops get on the lens.

The third problem is the identification of fog and precipitation types (e.g., rain, snow). Figure 12 shows that the variation of the estimated rainfall intensity of Camera 2 around 6:30 on October 13 was different from that of the observed rainfall intensity. The images from Camera 2 during this period were validated to be foggy in the selected patches. Therefore, the variation in the estimated rainfall intensity for Camera 2 can be attributed to the whitening of the background due to fog. Since this method estimates rainfall intensity from image whiteness, image whiteness caused by fog is misidentified as the effect of rainfall. At present, however, there is no method to determine whether it is fog or rain. Therefore, as a further study, it is necessary to investigate a method to determine whether the whiteness in the image under bad weather conditions is caused by rain or fog.

Finally, the fourth problem is the development of a nighttime rainfall estimation method. The method of this study is not applicable to nighttime images because it was difficult to distinguish rainfall. Therefore, rainfall estimation methods using nighttime images should be also considered separately. An idea for a rainfall estimation method using nighttime images is to use dynamic weather effects, such as counting the number of rain streaks that appear around the light source or near the lens, if the image is illuminated at night. Furthermore, recently, methods using infrared and near-infrared cameras to estimate rainfall intensity at night have also been proposed, and such methods can be utilized (Lee, 2023; Wang, 2023).
Thus, there are still several technical problems in the method of this study.

5. 4. 2 Possibility for practical use

The camera used in this study was a relatively inexpensive commercially available outdoor camera (approximately 300 US dollars per unit at the time of purchase), and cameras with similar performance have become even less expensive in recent years. Although the durability of the camera needs to be validated in the future, it is expected that data acquisition will be possible at the same level or lower cost than that of a classic tipping bucket rain gauge. Furthermore, cameras have already been installed outdoors for various purposes other than rainfall observation. The proposed method in this study can utilize images even without a special installation environment for rainfall observation purposes, as long as there is a certain distance to the background and the background is relatively undisturbed. In other words, it is expected that by effectively utilizing images from existing cameras, it will be possible to acquire a vast amount of rainfall data on the ground surface. Therefore, this technique potentially become a gap filler for areas in lacking surface rainfall observations. Moreover, if past images have been accumulated, it may be possible to go back in time and recover surface rainfall data. On the other hand, data processing time may be an issue in utilizing the data for real-time observations. However, the proposed method is extremely simple, requiring less than one minute to process one image using a typical commercial computer. Although we used the computer having specifications of 80 GB RAM and Intel core i7-10700 @2.90 GHz CPU in this study, such RAM capacity is not necessary for this process. In other words, it is considered that instantaneous rainfall intensity can be estimated with a time resolution of one minute or less using a typical commercial computer. Therefore, there is potential for various fields where rainfall observation can be effectively utilized, such as countermeasures against flash flood and debris flow, flood forecasting, and irrigation system operation, from a cost perspective. However, there are still several technical problems to be addressed to take advantage of this technique, as indicated in 5.4.1. Furthermore, there are concerns about privacy issues in the actual use of this method. In many outdoor surveillance cameras, it may be inevitable that persons will be captured. Therefore, when making data public, it is necessary to pay careful attention to privacy issues. Thus, it is important to understand that there are technical problems and privacy issues before practically using this method.”

[Related papers to add to the references]

- Lee, J., Byun, J., Baik, J., Jun, C., and Kim, H. J.: Estimation of raindrop size distribution and rain rate with infrared

surveillance camera in dark conditions, Atmos. Meas. Tech., 16, 707–725, https://doi.org/10.5194/amt-16-707-2023, 2023.
- Wang, X., Wang, M., Liu, X., Zhu, L., Shi, S., Glade, T., Chen, M., Xie, Y., Wu, Y., and He, Y.: Near-infrared surveillance video-based rain gauge, J. Hydrol., 618, 129173, https://doi.org/10.1016/j.jhydrol.2023.129173, 2023.

**< Comment 13 >**

- References are generally very good, but they need to be expanded and cite recent research related to the research topic. (The references must be recent, as there are many articles related to this topic that were published during this period).

Response:

We will cite some recent related research and add them to the references as follows.

Firstly, we will add the following sentence in L. 88.

"A lot of deep machine learning-based methods have been proposed in recent years as with the trend of studies about static weather effect (e.g., Lin et al., 2020; Lin et al., 2022; Yin et al., 2023; Zheng et al., 2023)."

[Related papers to add to the references]

- Lin, C. W., Lin, M. X., and Yang, S. H.: SOPNet Method for the Fine-Grained Measurement and Prediction of Precipitation Intensity Using Outdoor Surveillance Cameras, IEEE Access, 8, 188813–188824, https://doi.org/10.1109/Access.2020.3032430, 2020.
- Lin, C. W., Huang, X., Lin, M., and Hong, S.: SF-CNN: Signal Filtering Convolutional Neural Network for Precipitation Intensity Estimation, Sensors, 22(2), 511, https://doi.org/10.3390/s22020551, 2022.

Secondly, we will add the following sentence in L. 95.

"In particular, it has been pointed out that the limitation of deep machine learning-based methods is the lack of training data rather than the design of network structure and learning manners (Wang et al., 2021; Yan et al., 2023)."

[Related papers to add to the references]

- Wang, H., Yue, Z. S., Xie, Q., Zhao, Q., Zheng, Y., and Meng, D.: From Rain Generation to Rain Removal, Proc. CVPR. IEEE, 14786–14796, 2021
- Yan, K., Chen, H., Hu, L., Huang, K., Huang, Y., Wang, Z., Liu, B., Wang, J., and Guo, S.: A review of video-based rainfall measurement methods, WIREs Water, 2023;10:e1678., https://doi.org/10.1002/wat2.1678, 2023.

Thirdly, we will mention methods using infrared and near-infrared cameras to estimate rainfall intensity at night in recent years as shown in response to Comment 12.

[Related papers to add to the references]

- Lee, J., Byun, J., Baik, J., Jun, C., and Kim, H. J.: Estimation of raindrop size distribution and rain rate with infrared surveillance camera in dark conditions, Atmos. Meas. Tech., 16, 707–725, https://doi.org/10.5194/amt-16-707-2023, 2023.
- Wang, X., Wang, M., Liu, X., Zhu, L., Shi, S., Glade, T., Chen, M., Xie, Y., Wu, Y., and He, Y.: Near-infrared surveillance video-based rain gauge, J. Hydrol., 618, 129173, https://doi.org/10.1016/j.jhydrol.2023.129173, 2023.